Biochimica et Biophysica Acta, 1146 (1993) 213–218

BBAMEM 75855

Folding and dynamics of melittin in reversed micelles

Ettore Bismuto, Ivana Sirangelo and Gaetano Irace

Dipartimento di Biochimica e Biofisica, Università di Napoli, Naples (Italy)

(Received 22 July 1992)

Key words: Reversed micelle; Membrane–melittin interaction; Melittin folding; Frequency domain fluorometry; Fluorometry; Lifetime distribution

The main structural characteristics and the dynamic properties of melittin bound to the internal surface of reversed micelles, formed by sodium bis(2-ethyl-1-exyl)sulfosuccinate (AOT) in isooctane, were investigated by several spectroscopic techniques. Melittin has been found associated to reversed AOT micelles in a single state, thus indicating that this system behaves differently with respect to phospholipid vesicles where at least two forms of lipid associated melittin are observed. The dynamic properties of melittin in reversed AOT micelles at different water contents were examined by frequency domain fluorometry. The whole emission decay was analyzed in terms of lifetime distribution having a Lorentzian shape. The results indicated that the binding of melittin to inverted micelles determines an increase of emission heterogeneity compared to that observed for the fully extended helical monomer. This was explained in terms of a larger variety of microenvironmental conditions that the tryptophan residue experiences during its excited state. However, the conformation freedom of the peptide can be modulated by varying the micellar size.

Introduction

Melittin, the main toxic component of bee venom, is a cationic amphiphilic peptide consisting of 26 amino acids [1], which exhibits some unique structural characteristics. Because of its amphipathic character, melittin can exist in aqueous solution as either a monomer or a tetramer, depending on ionic strength and/or peptide concentration. At low ionic strength, the peptide is predominantly unfolded [2]. In the presence of high salt concentration, melittin self-associates forming a tetramer [3,4], in which each subunit is structurally organized as a bent α-helical rod, strongly amphiphilic [5,6]. In the tetramer, the non-polar side chains are extended mainly towards the inside of the bend [5,6]. The hydrophobic interactions, which occur among the non-polar sides of the helices, contribute to tetramer formation and its stabilization. A monomeric extended helical conformation has been observed for melittin in alcohol solution [7] or in aqueous solution containing a high concentration of $NaDodSO_4$[8].

The amphipathic character of the melittin helix is the most relevant factor in causing its tendency to strongly interact with cell membranes, sometimes determining membrane distruption and lysis [6]. Although there is a basic agreement about the similarity between the structure adopted by melittin upon its binding to a cell membrane and that present in the tetramer [9], the aggregation state and the peptide orientation within the lipid bilayers are still matter of debate. The insertion of melittin helix could occur with its axis perpendicular [9–12] or parallel [6,10,13] to the membrane plane. Recently, two forms of melittin, differing in the degree of tryptophan exposure to solvent, were detected upon binding to phospholipid vesicles [14] but it was unsolved whether the two forms corresponded to different aggregation states or different peptide orientations.

In the present study, we have examined the overall structural organization and the dynamics of the tryptophan microenvironment of melittin bound to reversed micelles formed by sodium bis(2-ethyl-1-exyl)sulfosuccinate (AOT), a widely used surfactant, in isooctane. Reversed AOT micelles represent a much simpler homogeneous system in comparison with the usually investigated membrane lipid bilayers. The structure of these aggregates is such that the polar headgroups of the surfactant molecules constitute the core of micelles while the hydrophobic tails extend towards the surrounding organic phase [15–19]. Reversed AOT micelles may include aqueous solutions of biopolymers

Correspondence to: G. Irace, Dipartimento di Biochimica e Biofisica, Università di Napoli, Via Costantinopoli 16, 80138 Napoli, Italy.

Abbreviations: AOT, sodium bis(2-ethyl-1-exyl)sulfosuccinate; CD, circular dichroism; $NaDodSO_4$, sodium dodecyl sulfate; DMPC, dimyristoyl-L-α-phosphatidylcholine.

such as proteins, enzymes and genetic material [20–26]. The properties of the water molecules entrapped in the polar core of reversed micelles are largely different from those of bulk water [27–30]. For these reasons, reversed micelles may represent an easily available membrane-bound water mimetic system for studying membrane–peptide interactions [3,31,32].

The results reported in this paper suggest that the state of melittin bound to the internal surface of reversed AOT micelles is unique, thus confirming that the system behaves in a much simpler manner with respect to DMPC vesicles where it has been shown that melittin is present in more than one single lipid associated state [14]. Moreover, the conformational freedom of the polypeptide appears to be modulated by the amount of water molecules constituting the micellar pool.

Materials and Methods

Melittin was purchased from Sigma (St. Louis, MO). The peptide concentration was determined spectrophotometrically with a Perkin-Elmer Lambda Array 3840 spectrophotometer. The molar absorption coefficient at 280 nm was assumed to be similar to that reported for the monomeric tryptophan residue (5570 $M^{-1}cm^{-1}$).

Chemicals. All common chemicals were reagent grade and were purchased from British Drug Houses. Sodium bis(2-ethyl-1-exyl)sulfosuccinate (AOT) and 2,2,4-trimethylpentane purchased from Sigma and Aldrich, respectively, were used without further purification. Double-distilled water was used for preparing reversed micelles samples.

Spectral measurements. Fluorescence measurements were made in the range where emission was linear with protein concentration. The absorbance of all samples was not exceeding 0.1 at the excitation wavelength. The temperature of the solution cell was maintained constant by using an external bath circulator (Weslab model LT50). Polarization measurements were performed with a Perkin-Elmer Model MPF-66 fluorescence spectrometer. The polarization was calculated from:

$$P = (I_{VV} - G \cdot I_{VH})/(I_{VV} + G \cdot I_{VH})$$

where $G = I_{HV}/I_{HH}$; I is the fluorescence intensity, and the first and the second subscript refer to the plane of polarization of the excitation and emission beams, i.e., V, vertical, and H, horizontal emission.

Circular dichroism measurements were carried out on a Jobin-Yvon MK3 spectropolarimeter, equipped with a temperature-controlled cell holder. The molar ellipticity [Θ], in units of deg cm^2 $dmol^{-1}$ was calculated by using a value of 115 as mean residue molecular weight. The circular dichroism spectra in the spectral region between 240 and 200 nm were analyzed in order to evaluate the amount of secondary structures as reported by Chang et al. [33] from X-ray data of 15 proteins. A IBM personal computer was used to perform the curve fitting.

Lifetime measurements. Lifetime measurements were performed by a multifrequency cross-correlation phase and modulation fluorometer (I.S.S., Urbana, IL) equipped with a 300 W xenon lamp. The absorbance of peptide was always lower than 0.1 at the exciting wavelength. The emission was observed through a long-wave pass filter (WG 330) with a cut-off wavelength at 330 nm to avoid Raman emission. The modulation frequency was variable from 1 to 200 MHz. A solution of *p*-terphenyl (from Kodak) in cyclohexane was placed in the reference cell to correct for color error [34]. A lifetime of 1.000 ns was assigned to the reference solution. Usually, not less than 15 different modulation frequencies were used, and the data were collected until the standard deviations from each measurements of phase and modulation were below 0.2° and 0.004, respectively. The sample temperature was measured prior to and after each measurement in the sample cuvette by using a digital thermometer (Omega, Model 410 B-TC).

A non-linear least-squares program from I.S.S. was used for lifetime analysis, minimizing the reduced chi-square [35–38] defined by the following expressions:

$$\chi^2 = \sum_{\omega} \frac{1}{\sigma^2_{\phi\omega}} (\phi_\omega - \phi_{c\omega})^2 + \sum_{\omega} \frac{1}{\sigma^2_{m\omega}} (m_\omega - m_{c\omega})^2 \quad (1)$$

$$\chi^2_{red} = \frac{\chi^2}{2N - \gamma - 1} \quad (2)$$

ω is the modulation frequency; $\sigma_{\phi\omega}$ and $\sigma_{m\omega}$ are the estimated standard deviations of measured phase angles and demodulations; ϕ_ω and $\phi_{c\omega}$ are the experimental and the calculated phase shifts; m_ω and $m_{c\omega}$ are the experimental and the calculated demodulation factors, respectively; N is the number of measurements for sample and γ is the number of free parameters. The experimental data were analyzed assuming a sum of lifetime exponentials or a continuous distribution defined only in the positive lifetime domain. Lifetime distributions are characterized by uniform (Eqn. 3), Gaussian (Eqn. 4) and Lorentzian (Eqn. 5) shapes:

$$f(\tau) = \begin{cases} \frac{1}{W}, \text{ for } C - W/2 \leqslant \tau \leqslant C + W/2 \\ 0, \text{ otherwise} \end{cases} \quad (3)$$

$$f(\tau) \propto e^{-4[(\tau - C)/W]^2 \ln 2} \quad (4)$$

$$f(\tau) \propto \left[1 + 4\left(\frac{\tau - C}{W}\right)^2\right]^{-1} \quad (5)$$

The essential fitting parameters are the center position (C) and the full width at half-maximum (W).

Results

Conformational properties of melittin in reversed AOT micelles

Prior to observing the tryptophan emission decay of melittin, we examined the effects produced on the intrinsic spectroscopic properties of melittin upon its inclusion in reversed AOT micelles of different size.

Fig. 1 shows the CD spectrum between 200 and 250 nm of melittin in reversed micelles having a H_2O/AOT molar ratio of 3.2. The presence of two characteristic minima at 209 and 220 nm indicates that melittin is largely organized in α-helical conformation under these experimental conditions. The CD spectrum, shown in Fig. 1, is almost superimposable to that reported by Kubota and Yang in the presence of a large excess of sodium dodecyl sulfate [8]. From their spectrum we could calculate the following mean residue ellipticities: $-25\,500$ and $-22\,500$ deg cm^2 dmol^{-1} at 208 and 222 nm, respectively. These values are somewhat larger than those we have observed for melittin in reversed AOT micelles, at the same wavelengths, i.e., $-21\,176$ and $-20\,415$ deg cm^2 dmol^{-1}, thus indicating a 5–10% loss of helical content which represent not even one complete helical turn. This would indicate that the helix content of melittin in inverted micelles decreases from 77% to about 70%. Moreover, the secondary structure of melittin was poorly influenced by varying the micelle size as indicated by the constancy of the mean residue ellipticity values at 208 and 222 nm (Table I).

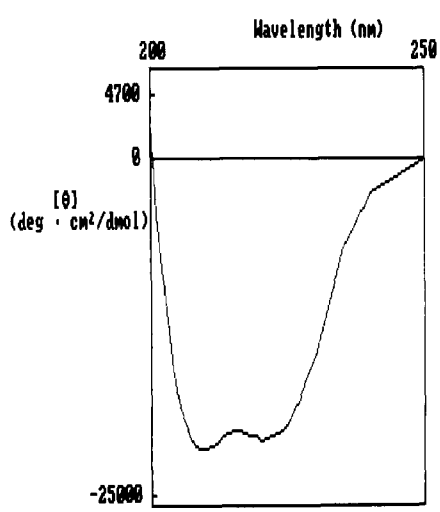

Fig. 1. Far ultraviolet CD spectrum of melittin in reversed micelles (H_2O/AOT molar ratio = 3.2) at 20°C.

TABLE I

Mean residue ellipticities at 208 and 222 nm of melittin in reversed micelles of different size

Determinations at 20°C. AOT content was 3% (w/v).

H_2O/AOT molar ratio	$[\Theta]_{208}$	$[\Theta]_{222}$
1.6	−21413	−20393
3.2	−21176	−20415
8.2	−21580	−20510

The steady-state emission spectra of melittin in reversed AOT micelles having a H_2O/AOT molar ratio of 3.2, obtained using different excitation wavelengths are shown in Fig. 2. The emission maximum was found centered in the wavelength range between 328 and 333 nm, thus indicating that the single tryptophan residue of melittin molecule is located in a rather non-polar hydrophobic environment; in fact, the emission maximum observed for the unorded melittin in salt free aqueous solution or in 6.0 M guanidine is at about 350 nm. The emission maximum of reversed AOT micelle bound melittin is also blue-shifted compared to that of the helical tetramer in aqueous solution, i.e., 341 nm [14,39]. The red-shift (about 5 nm) observed on increasing the excitation wavelength from 280 to 300 nm revealed the presence of emission heterogeneity, which can be ascribed to a selective excitation of differently oriented melittin molecules with respect to the negative charge of AOT molecules. A similar dependence was also found for melittin in reversed micelles of smaller as well as larger size.

The heterogeneity of the fluorescence emission of melittin in reversed AOT micelles of different size was further confirmed by observing the dependence of tryptophan steady-state polarization on wavelength emission. Fig. 3 shows such a dependence in comparison with that detected for the unordered monomer and

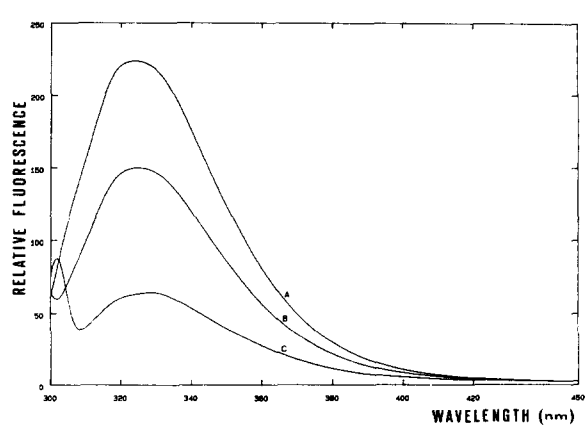

Fig. 2. Fluorescence emission spectra of melittin in reversed AOT micelles (H_2O/AOT molar ratio = 3.2) at 20°C. The excitation wavelengths were 280 nm (A), 295 nm (B), and 300 nm (C), respectively.

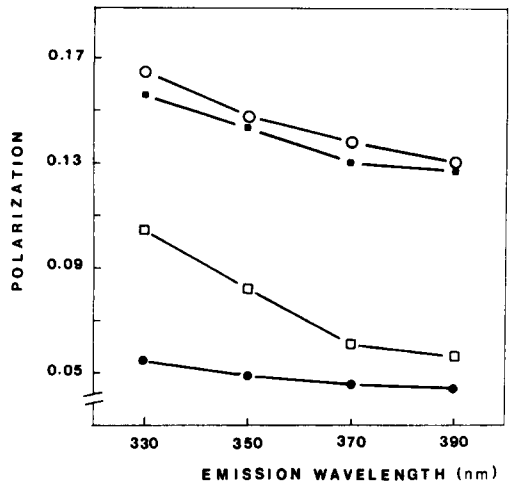

Fig. 3. Fluorescence polarization of melittin as function of emission wavelength: ●———●, unordered monomer; □———□, helical tetramer; ■———■ and ○———○ are relative to melittin in reverse micelles having 1.6 and 8.2 H_2O/AOT molar ratio, respectively.

helical tetramer. In the case of melittin bound to reversed AOT micelles as well as in the tetrameric state, the tryptophan polarization decreased on increasing the emission wavelength. As expected, the polarization at each emission wavelength depends on the aggregation state of melittin. In fact, the actual values of polarization followed the order: unordered monomer, ordered tetramer, and micelle-bound ordered monomer, thus reflecting the increase of rotational correlation time.

Frequency-domain emission decay of tetrameric and monomeric melittin

The tryptophan emission decay of melittin in different conformational states was examined by frequency domain fluorometry. The phase delays and demodulation factors, measured at modulation frequencies ranging from 1 to 140 MHz, were analyzed with the nonlinear least-squares routines described in Material and Methods. Different decay schemes, involving both discrete components and continuous unimodal Lorentzian distributions of fluorescence lifetimes, were used. In all cases, the fluorescence decays were poorly fitted in terms of a single lifetime component. Better fits were obtained using the bi-exponential model or continuous unimodal Lorentzian distributions of lifetimes. The results obtained for melittin at 15°C under various experimental conditions are shown in Table II. The unimodal distribution fits provided the lowest chi-square values except for the helical monomeric melittin in methanol; in fact, in this case, the emission decay was quite well represented as bi-exponential. However, the chi-squares relative to the distribution analysis were not sufficiently lower than those obtained with discrete biexponential fit in order to establish which

TABLE II

Discrete exponential and distribution analysis of monomeric unordered, monomeric helicoidal, and tetrameric helical melittin at 15°C

Melittin conformational state	Bi-exponential fit				Unimodal Lorentzian fit		
	f_1	τ_1 (ns)	τ_2 (ns)	χ^2	C (ns)	W (ns)	χ^2
Unordered monomer							
Water	0.79	4.48	1.70	3.76	3.89	1.53	2.96
6.0 M Gdn·HCl	0.89	3.94	1.40	2.54	3.69	1.15	2.36
Helical monomer							
Methanol	0.51	6.38	2.84	2.19	4.43	1.44	4.52
Helical tetramer							
	0.52	5.44	1.85	5.65	3.32	2.41	2.88

model has to be accepted [40]. We have recently shown that the biexponential fit of simulated data relative to a Lorentzian lifetime distribution with center at 3.0 ns and width of 1.0 ns provides a chi-square value which is only slightly higher than that obtained to fitting the same data to a Lorentzian distribution, i.e., 1.7 versus 1.3 [41]. Moreover, the existence of a correlation between the width of lifetime distribution and the length of polypeptide chain supports the choice of a distributional model [41].

Frequency-domain emission decay of melittin in reversed AOT micelles

Table III shows the fit parameters obtained from the analysis of the tryptophan emission decay of melittin in reversed micelles of different size at 15°C using the discrete biexponential model or continuous unimodal Lorentzian distributions of lifetimes. In all cases, the decays were well fitted in terms of unimodal Lorentzian lifetime distributions.

For melittin in reversed micelles of smallest size, i.e., AOT/water molar ratio of 3.2, the distribution width resulted considerably narrower compared to that observed for the peptide included in the largest vesicles. The increase of the vesicles size also produced a decrease of the distribution center from 3.12 ns to 2.57 ns.

TABLE III

Discrete exponential and distribution analysis of melittin in reversed AOT micelles

The excitation wavelength was 280 nm. Temperature was 15°C.

Molar ratio	Bi-exponential fit				Unimodal Lorentzian fit		
	f_1	τ_1 (ns)	τ_2 (ns)	χ^2	C (ns)	W (ns)	χ^2
3.2 H_2O/AOT	0.79	3.64	1.28	2.61	3.12	1.46	2.53
8.2	0.69	3.63	1.11	2.63	2.57	2.15	1.53

Discussion

The origin of a tryptophan lifetime distribution in peptides and proteins can be considered as resulting from two factors: the flexibility of the peptide backbone, which determines the existence of a large number of conformational substates, rapidly interconverting at room temperature, and the extreme sensitivity to the distinct microenvironment experienced by the indolic fluorophore during the excited state. Thus, if the tryptophan decay rates are faster than the interconversion rates among substates, the emission decay can be resolved in terms of a distribution of lifetimes [37,38, 42–44].

Bismuto et al. [43,45] observed that guanidine-induced unfolding of proteins increases the width of tryptophan lifetime distribution. This effect was explained assuming that the unfolded state possesses a larger variety of conformational substates which do not interconvert in the fluorophore lifetime scale.

The data reported in this paper show that the folding process that melittin undergoes on going from the unordered monomeric state (in salt free aqueous solution or in 6.0 M guanidine hydrochloride) to the helical monomeric state (in 80% methanol) dramatically changes the emission decay properties of the single tryptophan residue, i.e., Trp-19, contained in the peptide. In fact, the decay which is well represented by an unimodal Lorentzian distribution in the unordered monomer becomes bi-exponential in the fully extended helical form, thus indicating that the folding process reduces the emission heterogeneity.

Two factors may play an important role in making the indole microenvironment more homogeneous during the excited state: the poor flexibility of the helical rod and solvent effects. The former reduces the conformational space region accessible to the peptide segment containing the fluorophore. Therefore, the emission decay can be more simply considered as resulting from conformers about the C_α-C_β bond which differ for the rate of the charge transfer from the indole moiety to the closest positively charged groups along the helix axis. In this model, the solvent plays an important role in determining the amino acid conformations and the relative rates of interconversion among different rotamer populations.

The salt-induced self-association of melittin is known to determine a blue-shift of the emission maximum from 350 to 341 nm, thus indicating that the tryptophan residues are somewhat shielded from the solvent in the tetrameric form [14,39]. We have found that the tetramer formation strongly increases the emission heterogeneity, i.e., the tryptophan lifetime distribution of the tetrameric melittin becomes much broader than that observed for the unordered monomer. This result appears to contrast with the observation that the salt-induced association of melittin determines a folding of the molecule. In fact, a sharpening of lifetime distributions would be expected on protein folding [45,46]. However, it must be pointed out that the indole microenvironment in the tetramer originates from contact surface areas between four melittin helices [5,6]. In this case, each tryptophan residue can be regarded as an extrinsic fluorophore bound to the hydrophobic pocket formed by the remainder helices. Therefore, even if the folding that each subunit undergoes on going from the monomeric to the tetrameric state is expected to reduce the emission heterogeneity as observed in the case of helical monomer formation, the microenvironmental heterogeneity generated by structural fluctuations in the tetramer would broaden the fluorophore lifetime distribution. Broad lifetime distributions have been so far detected for naphthalensulfonates non-covalently bound to the heme pocket of apomyoglobin in comparison with those relative to the intrinsic indole residue which were found to be very narrow [43]. The presence of low amounts of tetramer in salt-free aqueous solution of melittin provides also an explanation for the larger distribution observed in this condition, i.e., $W = 1.53$, with respect to that detected in 6.0 M guanidine, i.e., $W = 1.15$.

The CD data presented in this paper indicate that melittin becomes largely helical on binding to synthetic inverted vesicles. At the same time, the indole residue comes in contact with the hydrophobic tails of AOT molecules as revealed from the significant blue-shift of the emission maximum from 350 to 325–328 nm. Moreover, the dependence of the position of the emission maximum on excitation wavelength is consistent with the occurrence of orientational dipolar relaxation processes occuring on nanosecond time scale [47]. This suggests that the indole residue of melittin is located in rather close proximity of AOT polar headgroups. The overall steady-state fluorescence characteristics of melittin in AOT reversed micelles correspond rather closely to those detected for the unquenchable fraction of the fluorescence emission of the same peptide bound to DMPC liposomes [14]. In fact, it has been shown that two lipid-associated forms of melittin can be detected on binding to DMPC vesicles: one, with the tryptophan residue exposed to the aqueous solvent and the other, penetrating the membrane interior, with the tryptophan residue located in close proximity to the phospholipid polar headgroups of the outer vesicles lipid layer. The results obtained on inverted micelles suggest that, in these systems, melittin exists in a single lipid-associated state, that we believe to be that corresponding to the form responsible for the unquenchable fraction of fluorescence emission observed in DMPC liposomes. Moreover, the observation that the lifetime distribution width of inverted micelle-bound melittin is significantly different from that observed for the helical

tetramer suggests that the peptide is monomeric under these experimental conditions. This is further confirmed by the position of the fluorescence emission maximum which is largely different from that observed for the tetrameric melittin. However, the fact that the fluorescence properties differ from those of the tetramer does not rule out the possibility that melittin is either dimeric or adopts some other associated state with geometrical features that differ from the tetramer.

The interpretation of the tryptophan fluorescence decay of melittin bound to synthetic inverted micelles in terms of continuous lifetime distribution can be related to the emission heterogeneity generated by a multitude of environmental conditions experienced by the fluorophore during the excited state. This could arise from different orientation that the tryptophan residue assumes with respect to the peptide backbone and the surrounding groups, i.e., water molecules, ionic head of AOT and hydrophobic tails of surfactants. The decrease of the distribution center observed on increasing the water content of the micellar pool can be related to a progressive enhancement of the internal micelle fluidity that facilitates the solvent dipolar relaxation around the excited state of the fluorophore. On the other hand, the increase of distribution width can be due to the larger variety of conformations which the peptide assumes because of the increased internal micellar fluidity. In this respect, it is interesting the observation that the lifetime distribution of a low molecular weight fluorophore, i.e., 1,8-anilinonaphthalenesulfonate (ANS), included in the water pool of reversed AOT micelles, becomes sharper on increasing temperature or micelle size as a consequence of the increased water mobility [48].

Acknowledgment

This work was supported by a CNR grant No. 90.01297.CT14.

References

1 Habermann, E. (1972) Science 177, 314–322.
2 Quay, S.C. and Condie, C.C. (1983) Biochemistry 22, 695–700.
3 Bello, J., Bello, H.R. and Granados, E. (1982) Biochemistry 21, 461–465.
4 Talbot, J.C., Dufourcq, J., De Bony, J., Faucon, J.F. and Lussan, C. (1978) FEBS Lett. 102, 191–193.
5 Terwilliger, T.C. and Eisenberg, D. (1982) J. Biol. Chem. 257, 6016.
6 Terwilliger, T.C., Weissman, L. and Eisenberg, D. (1982) Biophys. J. 37, 353–361.
7 Chen, Y.H., Yang, J.T. and Chan, K.H. (1974) Biochemistry 13, 3350.
8 Kubota, S. and Yang, J.T. (1986) Biopolymers 25, 1493–1504.
9 Vogel, H. and Jaehnig, F. (1986) Biophys. J. 50, 573–582.
10 Vogel, H. (1987) Biochemistry 26, 4562–4572.
11 Vogel, H., Jaehnig, F., Hoffmann, V. and Stumpel, J. (1983) Biochim. Biophys. Acta 733, 201–209.
12 Kempf, C., Klausner, R.D., Weinstein, J.N., Van Renswoude, J., Pincus, M. and Blumenthal, R. (1982) J. Biol. Chem. 257, 2469–2476.
13 Talbot, J.C., Faucon, J.F. and Dufourcq, J. (1987) Eur. Biophys. J. 15, 145–157.
14 Kaszycki, P. and Wasylewski, Z. (1990) Biochim. Biophys. Acta 1040, 337–345.
15 Menger, F.M., Saito, G., Sanzero, G.V. and Dodd, J.R. (1975) J. Am. Chem. Soc. 97, 909.
16 Israelachvili, J.N., Mitchell, D.J. and Ninham, B.W. (1976) J. Che. Soc. Faraday Trans. 2, 72, 1525.
17 Evans, D.F. and Ninham, B.W. (1986) J. Phys. Chem. 90, 226.
18 Eicke, H.F. and Parfitt, G.D. (1987) Interfacial Phenomena in Apsolan Media, Dekker, New York.
19 Luisi, P.L. and Straub, B. (1984) Reverse Micelle, Plenum Press, New York.
20 Luisi, P.L. (1985) Angew. Chem. 6, 449.
21 Martinek, K., Levashov, A.V., Klyachko, N., Khmelnitski, Y.L. and Berezin, I.V. (1986) Eur. J. Biochem. 155, 453.
22 Imre, V.E. and Luisi, P.L. (1982) Biochem. Biophys. Res. Commun. 107, 538.
23 Luthi, P. and Luisi, P.L. (1984) J. Am. Chem. Soc. 106, 7285.
24 Strambini, G.B. and Gonnelli, M. (1988) J. Phys. Chem. 92, 2850.
25 Brochette, P., Petit, C. and Pileni, M.P. (1988) J. Phys.Chem. 92, 3505.
26 Luisi, P.L. and Magid, L. (1986) J. CRC Crit. Biochem. 20, 409.
27 Douzou, P., Keh, E. and Balny, C. (1979) Proc. Natl. Acad. Sci. USA 76, 681.
28 Ali, S. and Bettelheim, F.A. (1985) Colloid. Polym. Sci. 263, 396.
29 Halle, B., Anderson, T., Forsen, S. and Lindman, B. (1981) J. Am. Chem. Soc. 103, 500.
30 Thompson, K.F. and Gierasck, L.M. (1984) J. Am. Chem. Soc. 106, 3648.
31 Grigolini, P. and Maestro, M. (1986) Chem. Phys. Lett. 127, 248.
32 Kim, V., Frolov, G.K., Ermakov, V.I. and Pak, S.E. (1987) Kolloidn. Zh. 49, 1067.
33 Chang, C.T., Wu, C.C. and Yang, J.T. (1978) Anal. Biochem. 91, 13–31.
34 Lakowicz, J.R., Cherek, H. and Balter, A. (1981) J. Biochem. Biophys. Methods 15, 131–146.
35 Gratton, E., Lakowicz, J.R., Maliwal, B., Cherek, H., Laczko, G. and Limkeman, M. (1984) Biophys. J. 46, 479.
36 Lakowicz, J.R., Laczko, G., Cherek, H., Gratton, E. and Limkeman, M. (1984) Biophys. J. 46, 463.
37 Alcalà, R., Gratton, E. and Prendergast, F.G. (1987) Biophys. J. 51, 597–604.
38 Alcalà, R., Gratton, E. and Prendergast, F.G. (1987) Biophys. J. 51, 925–936.
39 Quay, S.C. and Condie, C.C. (1983) Biochemistry 22, 695–700.
40 Brandt, S. (1976) Statistical and Computational Methods in Data Analysis, 2nd. Edn., North Holland, Amsterdam.
41 Bismuto, E., Sirangelo, I. and Irace, G. (1991) Arch. Biochem. Biophys. 291, 38–42.
42 Bismuto, E., Irace, G. and Gratton, E. (1989) Biochemistry 28, 1508–1512.
43 Bismuto, E., Sirangelo, I. and Irace, G. (1989) Biochemistry 28, 7542–7549.
44 Ferreira, S.T. (1989) Biochemistry 28, 10066–10072.
45 Bismuto, E., Gratton, E. and Irace, G. (1988) Biochemistry 27, 2132–2136.
46 Bismuto, E. and Irace, G. (1989) Photochem. Photobiol. 50, 165–168.
47 Demchenko, A.P. (1986) Ultraviolet Spectroscopy of Proteins, p. 320, Springer, Berlin.
48 Bismuto, E., Sirangelo, I. and Irace, G. (1992) Biophys. Chem. 44, 83–90.